A Framework of Optimal Remote Sensing using Small Unmanned Aircraft Systems

Brandon Stark[1], *Student Member, IEEE*, and YangQuan Chen[2], *Senior Member, IEEE*

***Abstract*—The use of small Unmanned Aircraft Systems (UAS) for remote sensing applications have increased significantly over the past decade. However, effective and efficient data collection methods and strategies are still being developed. The use of an effective small UAS methodology has become necessary, but it has additionally become important to also examine optimal remote sensing with respect to data quality. In this paper, a framework for the optimization of collecting remote sensing aerial imagery with small UAS is presented. Compared to other remote sensing techniques, the use of small UAS introduces several new tunable parameters that may have significant impact on data quality and the resulting analysis. The framework presented is a conceptual structure that describes optimal remote sensing with regard to the spatial, spectral, and temporal factors that provide the greatest signal-to-noise ratio for the desired application or purpose. Each of these factors are introduced and discussed as they pertain to a variety of parameters enabled by small UAS.**

I. Introduction

The development of small Unmanned Aircraft Systems (UAS) has grown dramatically over the past several years. Small UAS have been introduced in a wide variety of academic research projects, but their use is far from commonplace. There still remains many questions regarding their safety, practicality, and data reliability and repeatability. In addition, there remain a wide variety of platforms with no standardization and limited adaptability, which leads to limited options for scientific end-users [1]. Currently SUAS users must be both SUAS designers and researchers, leading to limited validation of data accuracy and ultimately limits the future of small UAS adoption.

One of the most promising applications of small UAS are in applications such as crop yield estimations, soil moisture monitoring, pest management, or soil salinity control that require a level of sensing robustness, reliability, and precision that many platforms are unable to satisfy. These applications are extensions of existing methodologies of traditional satellite or manned aircraft remote sensing applications that are well-established in literature. But given the unique advantages and challenges that are found with the use of small UAS, it is imperative to introduce new approaches to their usage.

In order to utilize small UAS remote sensing for the many applications, complex workflows and methodologies have been developed to obtain the best data. While technological advancement will lead to the standardization of the data results, existing standards on remote sensing accuracy and data already exist. As data has shifted into a primary small UAS objective, there has been an increased focus on data collection methodology and processing, especially tailored to small UAS [2]. The next stage for the small UAS remote sensing problem is addressing the optimality of data collection. Existing literature introduced optimal remote sensing strategies with respect to coverage control [3] or SUAS health [4]. In this paper, the focus is on the optimal remote sensing with respect to the optimality of the data.

The optimal remote sensing problem is based on the assumption that if any entity under investigation can be characterized by aggregate features, characteristics, and scale, then there must exist a measurement or range of measurements that provide the best representation of the entity. There then must exist a measurement that can be defined as the optimal measurement. This paper builds a conceptual framework for describing the optimality as a function of spatial, spectral, and temporal factors that provide the best representation.

The rest of the paper is organized as follows. Section II introduces the problem of remote sensing. Optimality of remote sensing is formulated in Section III. In Section IV, the optimality criterion is discussed in terms of each of the spatial, spectral, and temporal factors. Concluding remarks are presented in Section V.

II. SUAS Remote Sensing

Led by the development of small, high resolution cameras as well as suitable multi-spectral cameras, SUASs have demonstrated a significant level of capabilities for both agricultural and environmental applications [5]. There are large varieties of applications being investigated that are enabled by the high-resolution imagery provided by SUASs including irrigation timing control [6], canopy coverage and yield estimation [7], and disease and pest management [8]. Highly desirable metrics such as crop water stress estimation have also been investigated using SUASs [9]. Utilizing established remote sensing indices such as Normalized Difference Vegetation Index (NDVI) has also enabled a variety of applications valuable for agricultural such as yield estimation [10], and crop harvest yield attributes [11]. Multispectral indices such as Photochemical Reflectance Index (PRI) [12] as well as more complex analysis utilizing hyperspectral imagery [13] have also been demonstrated to be effective estimators for metrics such as water stress.

For environmental applications, rangeland management, including conservation efforts are also a prime example of the

[1]Mechatronics, Embedded Systems and Automation Lab, School of Engineering, University of California, Merced, Merced, CA, USA, bstark2@ucmerced.edu

[2]Mechatronics, Embedded Systems and Automation Lab, School of Engineering, University of California, Merced, Merced, CA, USA, ychen53@ucmerced.edu

978-1-5090-6190-7/16/$31.00

value of SUASs. The land classified as rangelands comprise of over half of the usable land in the world and have significant agricultural and economic value. Conservation and management of these lands can be a challenging task due to the wide variety of activity and large areas [14]. Satellite imagery can be used for decision support, but the resolution of the imagery is typically insufficient. Finer details such as individual vegetation and small water features are impossible to see and become difficult for management. Accurate assessment of small features, such as dead matter or litter have been identified as one of the most important indicators for assessing long-term sustainability of the land [15]. Current methods, using satellites or field-crews, suffer from high costs and limited actionable intelligence due to the sparse nature of the evaluations.

SUASs provide a new and cost efficient method for data collection for better rangeland management [15]–[17]. These autonomous systems have several advantages over satellite imagery or manned aircraft. They can fly at very low altitudes, enabling high resolution imagery, can accomplish a wide variety of mission and can be much safer and cheaper to operate. As a result, remote sensing applications for SUASs have seen significant growth as their utility gains credibility.

While there has been a recent interest of the agricultural implications of high-resolution or multi-spectral imagery, there remains a significant amount of work. Many of the solutions found in literature utilize specialized equipment, controlled environments, and rely on analysis expertise. These solutions are currently not implementable at any level of commercial operation and further development is necessary. The majority of existing methodology described in literature for SUASs was developed for low resolution satellite imagery or through the use of handheld hyperspectral sensors with high spectral resolution, meaning that these are not optimized for use by SUASs, which can provide high resolution imagery with limited spectral resolution and potentially with a higher temporal resolution. The true value of SUAS-based remote sensing may lie in the flexibility afforded by band-reconfigurable platforms working together [18].

A general form of the remote sensing problem can be described as follows. Let $\Omega \subset R^2$ be any arbitrary polytrope defining the area of interest. A series of band density functions η_λ are defined as $\eta_\lambda(q,t) \in [0,\infty) \forall q \in \Omega$, defining the spectral response at any point q of size δ^2 in the region for a spectral wavelength λ, at any time $t \in [t_1, t_2]$. To this affect, the usefulness of a mapping from Ω to a given number of η_λ bands is dependent on the proper selection of spatial resolution δ, spectral bands λ, and temporal resolution t.

III. Optimality in Remote Sensing

If an entity can be represented in terms of aggregate features, characteristics, and scale, then there must exist a measurement that provides the 'best' representation. This optimality can be defined using the definition of remote sensing described in Section II. By extension, there must exist some values of δ, λ, and t that provide the optimal η bands that provide the optimal representation of the entity of interest. It is then the goal of optimal remote sensing to obtain these factors to obtain the best representation given the constraints and limitations afforded by the platform.

TABLE I: Optimality Criterion Arguments

Flight Parameters	**Sensor**	**Environmental**
Flight Alt. (h)	Resolution. (P)	Scale of Interest
Flight Spacing	Pixel Pitch (PP)	System Dynamics
Time of Day	Pixel Size (PS)	Weather Conditions
Flight Patterns	Focal Length (F)	
Airspeed	Spectral Sensitivity	
Overlap %	Interval t_{sensor}	

Remote sensing optimality must be described with respect to the minimization of an optimality criterion and subject to the technical and physical constraints of the implementation. In this paper, the minimization of the optimality criterion is described by

$$\min_{u \in \mathcal{U}} J = \left| \frac{cost(x,u)}{performance(x,u)} \right| + \phi[x_0, u_0] \tag{1}$$

where $cost(x,u)$ and $performance(x,u)$ are some arbitrary cost and performance function of SUAS remote sensing at state x, and input u. The state x includes, but is not limited to the aircraft position or other internal states related to the payload and the environment. The set $\mathcal{U}$ contains, but is not limited to the parameters listed in Tab. I, and $\phi[x_0, u_0]$ describe the initial conditions at state x_0 and initial parameters u_0.

The optimal remote sensing control law π then satisfies

$$\pi = \arg\min_{u \in \mathcal{U}} \left\{ \left| \frac{cost(x,u)}{performance(x,u)} \right| + \phi[x_0, u_0] \right\} \tag{2}$$

However, there is no uniqueness to the control law solution. The minimum in the optimal remote sensing may be achieved for multiple arguments in set $\mathcal{U}$. Thus there may exist multiple solutions for an optimal remote sensing operation.

In order to understand the optimality in terms of δ, λ, and t, $cost(x,u)$ is described as a weighted product of $cost_\delta$, $cost_\lambda$, and $cost_t$ for a given value of δ, λ, and t. This can be represented as

$$cost(x,u) = \prod_{i \in [\delta,\lambda,t]} \alpha_i \cdot cost_i(x,u) \tag{3}$$

where α_i is an arbitrary weight specified by the remote sensing application. Likewise, $performance(x,u)$ can be described as

$$performance(x,u) = \prod_{i \in [\delta,\lambda,t]} \alpha_i \cdot performance_i(x,u) \tag{4}$$

The minimization equation can be rewritten as

$$\min_{u \in \mathcal{U}} J = \prod_{i \in [\delta,\lambda,t]} \left| \frac{\alpha_i \cdot cost_i(x,u)}{performance_i(x,u)} \right| + \phi[x_0, u_0] \tag{5}$$

It can be seen that (5) may be rewritten as some function of δ, λ, and t, such that for a solution space $J(x,u)$ there exists a mapping T where $T : J(x,u) \leftrightarrow S(\delta, \lambda, t)$.

IV. Optimality Criterion for Remote Sensing

From the description of optimality in remote sensing, it can be seen that it is comprised of the optimization of spatial, spectral, and temporal factors. In this section, each of these factors are discussed in detail.

A. Spatial Resolution

In remote sensing imagery, the spatial sampling scale is a fundamental aspect to analysis as well described in literature [19]. Simply put, if an object can be characterized by visible features, then there must exist some optimal spatial resolution at which corresponds to the scale and aggregation level characteristic of the geographical entity of interest. This definition and corresponding methodology, requires the need for a predefined geographical entity of interest and *a priori* identification of the aggregate data that optimally defines the entity of interest. This is not a trivial step, and is key to a sufficient small UAS remote sensing methodology [1].

While higher spatial resolution may always be preferred, there are many associated costs. Unlike a satellite, a small UAS has the ability to maneuver to a desired altitude to provide a chosen spatial resolution though it may have an effect on flight performance or limited by boundary conditions. The spatial resolution, or ground sampling distance (GSD) is a function of the image footprint (FP) and sensor resolution (P), and is given by

$$GSD = \frac{FP}{P} \tag{6}$$

where FP is given by

$$FP = \frac{h \cdot PP \cdot PS}{F} \tag{7}$$

where h is the flight altitude above ground level, PP is the sensor's pixel pitch, PS is the sensor's pixel size, and F is the sensor's focal length.

Boundary conditions typically constrain the set of sensor parameters (P, PS, PP, F) given a limited number of available sensors and technology.

However, as flight altitude decreases, so does the image footprint FP which may impact total flight coverage given a finite flight endurance, necessitating a need to optimize. The following set of equations (8-11) can be used as constraining equations during optimization to describe the flight spacing (S), Mission Time (MT), Max Area (A_{max}), or Max Airspeed (v_{max}) of a small UAS Remote Sensing application for a given parameters of the sensor and desired performance:

$$spacing = FP \cdot (1 - overlap) \tag{8}$$

$$MissionTime = time_{track} \cdot n_{tracks} \tag{9}$$

$$MaxArea = v \cdot spacing \cdot MT \tag{10}$$

$$MaxAirspeed = \frac{FP_{vert} \cdot (1 - overlap)}{t_{sensor}} \tag{11}$$

where $spacing$ is the spacing between parallel flight tracks, $overlap$ is the desired image overlap percentage, $time_{track}$ is the flight time per track, n_{tracks} is the number of needed flight tracks to cover an area, v is the small UAS's airspeed, and t_{sensor} is the sensor's set imaging interval.

TABLE II: Common Vegetation Indices

Indices	**Formula**
Normalized Difference VI (NDVI)	$\frac{\rho_{(800+\Delta)} - \rho_{(680+\Delta)}}{\rho_{(800+\Delta)} + \rho_{(680+\Delta)}}$
Green NDVI	$\frac{\rho_{(800+\Delta)} - \rho_{(550+\Delta)}}{\rho_{(800+\Delta)} + \rho_{(550+\Delta)}}$
Normalized Difference Water Index (NDWI)	$\frac{\rho_{(980+\Delta)} - \rho_{(1240+\Delta)}}{\rho_{(980+\Delta)} + \rho_{(1240+\Delta)}}$
Photochemical reflectance index (PRI)	$\frac{\rho_{570} - \rho_{531}}{\rho_{570} + \rho_{531}}$

B. Spectral Resolution

Spectral optimization is a similar condition as spatial optimization. If there exists spectral characteristics that can uniquely define an object, then there must exist an optimal spectral resolution of which to view the spectral characteristics. As with spatial resolution, there are methodologies presented in literature to define optimal spectral resolutions and optimal spectral measurements [20]–[22]. Much like spatial optimization, spectral optimization is related to the spectral separability of the desired entity of interest and the minimization of perturbing features of external factors such as atmospheric disturbance and soil reflectance.

As in spatial optimization, *a priori* knowledge of the spectrum of the entity of interest is required. Fig 1. depicts spectral reflectance across a range of wavelengths corresponding to visible and near infrared light. Many relationships of biophysical properties and spectral reflectances have been identified in literature, and many Vegetation Indices (VI) have been developed as a result [22], utilizing a wide array of different spectral wavelengths. Four common VI's can be found in Tab. II, where the number specifies the central spectral wavelength in μm. The Δ signifies the variability within the λ bandwidth that may be a tunable parameter.

The most common vegetation indices utilize the response in the red and near-infrared regions of the spectrum. As seen in Fig. 1, the sharp difference in reflectance between the two spectrums in vegetation is significant compared to the gradual spectral variation in soil or dead grass. These relationships, form the basis of optimal spectral remote sensing, especially realized in the form of narrow-band vegation indices [22].

However, unlike spatial optimization, spectral optimization has a limited number of degrees of freedom. Commercially available off-the-shelf cameras collect broadband measurements in three channels that obscure fine spectral details. Scientific imagers have been developed for small UAS to mimic the effect of satellite measurements, however suffer from limited options. Hyperspectral imagers, such that are

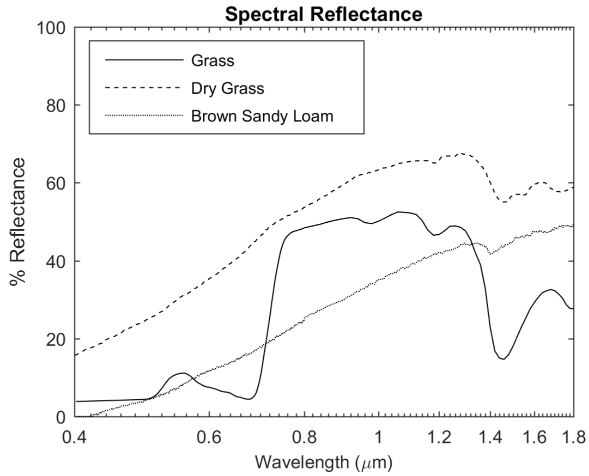

Fig. 1: Spectral reflectance in the visible and near-infrared region. Data courtesy of ASTER [23].

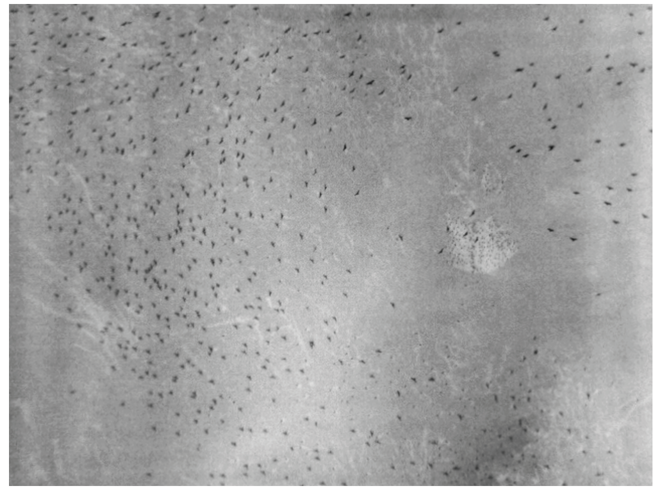

Fig. 2: The waterfowl appear colder than the warm water, though the temperature difference is only a few degrees.

needed for narrow-band indices, are not readily available for small UAS due to their cost and weight. In this aspect, spectral optimization may be temporarily limited by technological boundary conditions. However, physical boundary conditions, such as the limitations of analysis techniques for certain vegetation biophysical properties are more difficult to address and to optimize.

C. Temporal Resolution

The concept of finely optimizing the temporal resolution is unique to small UASs. Unlike other remote sensing technology, data collection with a small UAS may be finely controlled, enabling a fine control previously unrealizable. The temporal scale for data collection with a small UAS may be over the course of a year or as small as over the course of an afternoon or shorter. Literature has remarked on this ability to collect finely controlled aerial data by collecting multiple data sets in a day [24] or optimizing data collection for a specific time [25]. The optimization of the temporal axis may be deployed as a means to minimize identification overlap or to show the changes of a system dynamic over time.

In image classification applications, it has been well documented that shadowed objects impede classification efforts. Thus the optimal time for data collection can be defined as the point in which the shadows are minimized (12): [25]

$$\underset{t\in[t_1,t_2]}{\arg\min}\, Shadow(q,t) \quad \forall q \in \Omega \tag{12}$$

where $Shadow(q,t)$ is a binary map of the existance of a shadow at point q at time t. The time t of minimization may be close, though not identical to solar noon due to the topography of the region Ω [25].

Optimization along the temporal axis may also be seen in an example of utilizing a thermal camera for the counting of waterfowl over a marshland at night. The regular and accurate count of waterfowl is an important aspect in wetland conservation and as these birds roost at night over water, they are only visible to thermal imaging. The thermal capacitance of the water retain heat better than the waterfowl in the cold air, resulting in the birds appearing colder than the warm water (Fig 2). The optimal time for thermal data collection can be described as the time at which the difference between the water and the waterfowl is maximized.

While a small UAS may be more finely flexible in the time of data collection, there are several boundary conditions. Unlike a satellite, the time it takes for a small UAS to collect the necessary aerial imagery is not trivial. Flights with a fixed-wing small UAS may take as long as 1 to 2 hours, limiting the temporal bandwidth of data collection. On the other hand, rotary-wing vehicles typically suffer from significantly reduced flight times, generally on the order of 15-20 minutes. These factors provide strict limitations on the total availability of the data.

D. Boundary Conditions

Boundary conditions play a major role in the optimization of remote sensing. In a small UAS setting, these boundary conditions generally occur in two forms: technological constraints and physical constraints.

Technological constraints include many associated directly with the selection of the small UAS platform and sensor. These conditions include limitations on total flight endurance, minimum/maximum airspeeds, sensor resolution, sensor rate and sensor spectral sensitivity. While there exists some flexibility in the selection of these parameters, certain values may not be available, such as in the previous discussion of sensor resolution. As technology improves, these boundary conditions may loosen and enable more optimal solutions. Pixel counts in small UAS imaging systems has continued to improve over the past several years, enabling higher and higher image resolution (Tab. III). On the other hand, physical constraints, such as those related to system dynamics of the entity of interest, pose

TABLE III: Sensor Resolution relationship with Sampling Resolution

Sensor MP	Pixel Count	GSD	Year Introduced
4MP	2240 x 1680	7.00 cm	2001
10 MP	3681 x 2734	4.26 cm	2008
20 MP	5184 x 3888	3.02 cm	2012

significant challenges and are one of the major drivers for the investigation of optimal remote sensing.

V. Conclusion

The proposed conceptual framework establishes three major factors that can be optimized to generate the parameters (Tab. I) for optimal remote sensing with a small UAS. While data storage may be relatively inexpensive, collecting optimal data could improve data processing, or reduce operating costs. However, the implementation of optimal data collection is not trivial and highly application dependent. This conceptual structure highlights that many parameter relationships have yet to be developed or generalized. This does not imply that considering optimality is not of value, but rather indicates that there the current use of a small UAS for remote sensing is still in its infancy and there is more still yet to be explored.

An aspect that has not been fully explored is in the case of time-varying optimization in spatial or spectral factors. Consider a case where the remote sensing goal is not uniform across the region Ω, instead the desired δ is spatially dependent or the desired η band mapping of λ varies with t. Unlike traditional remote sensing, a small UAS or a fleet of small UAS, may be developed in such a manner where the data collection could be optimal at every point q instead of optimal for the region Ω.

This framework may also be advantageous in the expansion to $\Omega \in R^3$. Incorporating three dimensional spatial, spectral, and temporal data into the remote sensing framework has also recently started to gain traction and small UAS are poised to become significant data generators for spatially complex areas. The value of optimal data collection will become even greater with an additional dimension of spatial data collection that may exponentially increase data processing and analysis time unless properly accomplished.

As more small UAS are utilized in remote sensing applications, issues of methodology and optimal data collection will become more prevalent. A small SUAS can provide many advantages, but also has many unique challenges that need to be addressed before they can be used reliably and repeatedly. The conceptual framework presented is organized around a mapping of optimal remote sensing into spatial, spectral, and temporal factors to generate the parameters that provide the optimal data. In practice, boundary conditions may play significant roles in limiting the set of solutions, however, many technical barriers may be significantly reduced over time.

References

[1] B. Stark, B. Smith, and Y. Chen, "A guide for selecting Small Unmanned Aerial Systems for scientific research applications," in *Research, Education and Development of Unmanned Aerial Systems*, vol. 2, pp. 38–45, 2013.

[2] B. Stark and Y. Q. Chen, "Remote Sensing Methodology for Unmanned Aerial Systems," in *Encyclopedia of Aerospace Engineering - UAS* (R. Blockley and W. Shyy, eds.), Wiley, 2016.

[3] H. Chao and Y. Chen, *Remote Sensing and Actuation Using Unmanned Vehicles*. John Wiley & Sons, 2012.

[4] B. Stark, S. Rider, and Y. Chen, "Optimal Control of a Diffusion Process Using Networked Unmanned Aerial Systems with Smart Health," in *World Congress*, vol. 19, pp. 1254–1259, 2014.

[5] C. Zhang and J. M. Kovacs, "The application of small unmanned aerial systems for precision agriculture: a review," *Precision agriculture*, vol. 13, no. 6, pp. 693–712, 2012.

[6] J. Baluja, M. P. Diago, P. Balda, R. Zorer, F. Meggio, F. Morales, and J. Tardaguila, "Assessment of vineyard water status variability by thermal and multispectral imagery using an unmanned aerial vehicle (uav)," *Irrigation Science*, vol. 30, no. 6, pp. 511–522, 2012.

[7] J. I. Córcoles, J. F. Ortega, D. Hernández, and M. A. Moreno, "Estimation of leaf area index in onion (allium cepa l.) using an unmanned aerial vehicle," *Biosystems Engineering*, vol. 115, no. 1, pp. 31–42, 2013.

[8] F. Garcia-Ruiz, S. Sankaran, J. M. Maja, W. S. Lee, J. Rasmussen, and R. Ehsani, "Comparison of two aerial imaging platforms for identification of huanglongbing-infected citrus trees," *Computers and Electronics in Agriculture*, vol. 91, pp. 106–115, 2013.

[9] V. Gonzalez-Dugo, P. Zarco-Tejada, J. A. Berni, L. Suárez, D. Goldhamer, and E. Fereres, "Almond tree canopy temperature reveals intra-crown variability that is water stress-dependent," *Agricultural and Forest Meteorology*, vol. 154, pp. 156–165, 2012.

[10] K. C. Swain, S. J. Thomson, and H. P. Jayasuriya, "Adoption of an unmanned helicopter for low-altitude remote sensing to estimate yield and total biomass of a rice crop," *Transactions of the ASAE (American Society of Agricultural Engineers)*, vol. 53, no. 1, p. 21, 2010.

[11] T. Jensen, A. Apan, F. Young, and L. Zeller, "Detecting the attributes of a wheat crop using digital imagery acquired from a low-altitude platform," *Computers and Electronics in Agriculture*, vol. 59, no. 1, pp. 66–77, 2007.

[12] P. J. Zarco-Tejada, V. González-Dugo, L. Williams, L. Suárez, J. A. Berni, D. Goldhamer, and E. Fereres, "A PRI-based water stress index combining structural and chlorophyll effects: Assessment using diurnal narrow-band airborne imagery and the CWSI thermal index," *Remote sensing of environment*, vol. 138, pp. 38–50, 2013.

[13] P. J. Zarco-Tejada, M. Guillén-Climent, R. Hernández-Clemente, A. Catalina, M. González, and P. Martín, "Estimating leaf carotenoid content in vineyards using high resolution hyperspectral imagery acquired from an unmanned aerial vehicle (UAV)," *Agricultural and Forest Meteorology*, vol. 171, pp. 281–294, 2013.

[14] P. J. Hardin and M. W. Jackson, "An Unmanned Aerial Vehicle for Rangeland Photography," *Rangeland Ecology & Management*, vol. 58, no. 4, pp. 439–442, 2005.

[15] R. P. Breckenridge, M. Dakins, S. Bunting, J. L. Harbour, and S. White, "Comparison of unmanned aerial vehicle platforms for assessing vegetation cover in Sagebrush Steppe ecosystems," *Rangeland Ecology & Management*, vol. 64, no. 5, pp. 521–532, 2011.

[16] J. J. Mitchell, N. F. Glenn, M. O. Anderson, R. C. Hruska, A. Halford, C. Baun, and N. Nydegger, "Unmanned Aerial Vehicle (UAV) Hyperspectral Remote Sensing for Dryland Vegetation Monitoring," in *Proc. of Whispers 4th Workshop on Hyperspectral Image and Signal Processing: Evolution in Remote Sensing*, 2012.

[17] A. S. Laliberte, J. E. Herrick, A. Rango, and C. Winters, "Acquisition, orthorectification, and object-based classification of unmanned aerial vehicle (UAV) imagery for rangeland monitoring," *Photogrammetric Engineering and Remote Sensing*, vol. 76, no. 6, pp. 661–672, 2010.

[18] H. Chao, M. Baumann, A. Jensen, Y. Chen, Y. Cao, W. Ren, and M. McKee, "Band-reconfigurable multi-UAV-based cooperative remote sensing for real-time water management and distributed irrigation control," in *IFAC World Congress, Seoul, Korea*, 2008.

[19] D. J. Marceau, D. J. Gratton, R. A. Fournier, and J.-P. Fortin, "Remote sensing and the measurement of geographical entities in a forested environment. 2. The optimal spatial resolution," *Remote Sensing of Environment*, vol. 49, no. 2, pp. 105–117, 1994.

[20] M. M. Verstraete and B. Pinty, "Designing optimal spectral indexes for remote sensing applications," *Geoscience and Remote Sensing, IEEE Transactions on*, vol. 34, no. 5, pp. 1254–1265, 1996.

[21] A. L. Nguy-Robertson, Y. Peng, A. A. Gitelson, T. J. Arkebauer, A. Pimstein, I. Herrmann, A. Karnieli, D. C. Rundquist, and D. J. Bonfil, "Estimating green LAI in four crops: Potential of determining optimal spectral bands for a universal algorithm," *Agricultural and forest meteorology*, vol. 192, pp. 140–148, 2014.

[22] H. G. Jones and R. A. Vaughan, *Remote Sensing of Vegetation*. Oxford University Press, New York, USA, 2010.

[23] A. Baldridge, S. Hook, C. Grove, and G. Rivera, "The ASTER spectral library version 2.0," *Remote Sensing of Environment*, vol. 113, no. 4, pp. 711–715, 2009.

[24] J. A. Berni, P. J. Zarco-Tejada, L. Suárez, and E. Fereres, "Thermal and narrowband multispectral remote sensing for vegetation monitoring from an Unmanned Aerial Vehicle," *Geoscience and Remote Sensing, IEEE Transactions on*, vol. 47, no. 3, pp. 722–738, 2009.

[25] B. Stark and Y. Chen, "Optimal Collection of High Resolution Aerial Imagery with Unmanned Aerial Systems," in *Unmanned Aircraft Systems (ICUAS), 2014 International Conference on*, pp. 89–94, IEEE, 2014.